JOURNAL OF SOLID STATE CHEMISTRY **104**, 88–98 (1993)

Hydrolysis of Lanthanide Dicarbides: Rates of Reaction of Cubic and Tetragonal Solid Solutions with Water

I. J. McCOLM

Department of Industrial Technology, University of Bradford, BD7 1DP, United Kingdom

Received October 29, 1992; accepted November 9, 1992

Two series of solid solutions, $Ho_{1-x}La_xC_2$ and $Nd_{1-x}LaC_2$, have been made and their X-ray unit cell parameters measured. The $Ho_{1-x}La_xC_2$ series contains two tetragonal phases and a cubic solid solution series which has enabled the reaction rate constants for the water hydrolysis reaction of a cubic dicarbide phase to be determined for the first time. By comparing the linear rate constants and the activation energies across the two series the nature of bonding in general and the structure of the cubic phase are elucidated. A comparison with microhardness data is made and the change in M–C_2 bonding as a function of composition is considered. © 1993 Academic Press, Inc.

Introduction

J. S. Anderson *et al.* (*1*) developed the mild hydrolysis technique as an aid to structural and nonstoichiometric studies of lanthanide and actinide carbides and they were able to show the possibilities of isomorphous replacement of O^{2-} ions by C_2^{2-} ions in rare earth oxides (*2*). Hydrocarbon product distribution arising from the primary reactions set out in Eqs. [1], [2], and [3] was the key to the work but at the time no consideration was given to the kinetics of the reaction. Recently (*3, 4*), the kinetics of both water vapor and water reactions of the dicarbides have been measured while endeavouring to remain within the "mild conditions" defined by Anderson *et al.* (*1*), and the data have been considered in the light of possible solid state bonding models in these hard, refractory compounds which exhibit elements of covalent, ionic, and metallic bonding.

The lanthanide dicarbides are all polymorphic, having a high temperature cubic phase which transforms to a tetragonal form on cooling below 1000–1500°C, depending on the system studied. Attempts to quench the cubic phase to room temperature (*5*), or otherwise stabilize it (*2*), by Anderson and coworkers were not successful. Later this was achieved by forming solid solutions between LnC_2 and $Ln'C_2$ carbides that had a greater than critical cell volume size difference (*6, 7*). This paper reports results obtained for some cubic dicarbides, the necessary investigations of which J. S. Anderson was himself responsible for setting in progress, but which took many years to eventually complete; the kinetics of hydrolysis of cubic dicarbide phases is reported for the first time. Data on the products of hydrolysis and the rates of hydrolysis of LaC_2–HoC_2 and LaC_2–NdC_2 solid solutions are reported for both cubic and tetragonal phases and are discussed in the light of results in our earlier publications (*3, 4*).

In order to conform to the strict definition

0022-4596/93 $5.00

of mild hydrolysis the reactions stated as Eqs. [2] and [3] should be studied using water vapor as the reagent at temperatures below 40°C; but while this gives the hydrocarbon product distribution characteristic of the C_n^{x-} species present in the solid, the rate-limiting step is the surface concentration of H_2O, which makes kinetic parameter evaluation of limited value (*3*). Hence the kinetic parameters were found by immersing small arc-melted beads in water and using an evolved gas manometric method to measure the reaction rate. First, several measurements on a series of solid solutions had to be obtained to show that the secondary reactions, Eq. [3], removed a relatively constant volume of the primary product gases.

Correlation between x-ray unit cell volumes, hardness, and the linear reaction rate constant were observed and an increased reactivity of the cubic phase compared to tetragonal polymorphs was deduced. These investigations do help somewhat toward solving the question of the structure of the cubic phase.

It has been suggested that the high temperature polymorph becomes cubic due to rotation of the C_n^{2-} anions along the $\langle 111 \rangle$ crystallographic directions of the unit cell as opposed to parallel alignment along the *c*-axis direction as in the tetragonal phase.

The hydrolysis reactions are summarized as

$$M^{III}C_2 + 3H_2O = M(OH)_3 + C_2H_2 + \tfrac{1}{2}H_2 \qquad [1]$$

$$M^{IV}C_2 + 4H_2O = M(OH)_4 + C_2H_2 + H_2. \qquad [2]$$

Several reactions responsible for removing hydrogen and actylene from the product mixture are given as

$$\begin{aligned} C_2H_2 + H_2 &= C_2H_4 \\ C_2H_2 + 2H_2 &= C_2H_6 \\ 2C_2H_4 + H_2 &= C_4H_6 \\ n\,C_2H_4 &= \text{solid wax.} \end{aligned} \qquad [3]$$

Experimental

The dicarbides were prepared and characterized as described previously (*7*) and from these the dicarbide solid solutions, $Ln_{1-x}Ln_x^1C_2$; were prepared and characterized as described in (*3*).

An all-glass water-manometer system which was a modified version of that shown in Ref. (*8*) was used. The double-walled manometer and reaction vessel were maintained at a constant temperature by pumping water around the hollow walls using a Shandon constant temperature circulator. As the reaction proceeded the increased pressure in the apparatus from the C_2H_2 and H_2 was observed as a depression of the water level in the manometer side arm by using a cathetometer with cross-wires focused on the water meniscus. A typical experiment involved sealing a small arc-melted bead of 25 mg mass, together with an iron rod, in an evacuated Pyrex glass bulb. This bulb was suspended within the hollow glass vacuum tap at the top of the reaction tube by a magnet at the outside. The reaction tube containing the water and manometer was then evacuated and allowed to come to equilibrium, which usually took about 2 hr. After equilibration the magnet was removed, the bulb fell into the reaction vessel and broke, and hydrolysis began. From this point the increase in the water level was noted. Specimen temperatures were maintained by immersing the reaction tube in a water bath maintained at the required temperature. Before sealing each bead was weighed and the dimensions were determined using a micrometer and a microscope with a scale eyepiece.

The rate data were obtained as a height decrease in the water column with time for unit surface area: "cm" $cm^{-2}\,min^{-1}$. Three to seven runs per sample were done in order to obtain the average values quoted in the results. The maximum deviation was generally found to be within ∓ 15% in a series of seven samples of each dicarbide. Where a

TABLE I

HYDROLYSIS PRODUCTS OBTAINED WHEN DICARBIDE PHASES ARE REACTED AT 293 K WITH WATER VAPOR AT 11.0 × 10^2Nm^{-2}

Product/ compound %	$La_{0.5}Lu_{0.5}C_2$ cubic	Annealed $La_{0.5}Lu_{0.5}C_2$ cubic	$Ce_{0.5}Er_{0.5}C_2$ cubic	$La_{0.5}Ho_{0.5}C_2$ cubic	LaC_2 tet.	NdC_2 tet.	HoC_2 tet.
CH_4	0.11	0.10	0.03	0.12	0.24	0.11	0.90
C_2H_6	5.2	1.3	2.7	4.6	6.77	7.27	1.80
C_2H_4	2.5	2.2	2.7	2.8	2.54	7.85	5.21
C_2H_2	92.2	96.5	94.6	92.4	89.5	85.0	92.1
C_3H_8	—	—	—	—	0.14	—	—

TABLE II

EXPECTED AND MEASURED GAS VOLUMES AT 293 K FOR THE REACTION OF DICARBIDE SOLID SOLUTIONS WITH WATER

Sample	*Structure*	Observed Vol. V_o (*cm*^{3})	Expected Vol. V_e (*cm*^{3})	V_o/V_e
$Lu_{0.95}La_{0.05}C_2$	cubic	2.2	4.2	0.52
$Lu_{0.1}La_{0.9}C_2$	"	1.3	2.6	0.50
$Lu_{0.5}La_{0.5}C_2$	"	3.3	6.4	0.52
$Gd_{0.3}Er_{0.7}C_2$	tet.	2.3	4.7	0.49
$Gd_{0.50}Er_{0.5}C_2$	"	1.7	3.6	0.49
$Gd_{0.6}Er_{0.4}C_2$	"	2.4	4.5	0.53
$Gd_{0.9}Er_{0.1}C_2$	"	1.9	3.9	0.48
$Ce_{0.50}Lu_{0.5}C_2$	cubic	2.2	4.5	0.49
$Nd_{0.50}Lu_{0.5}C_2$	"	2.3	4.4	0.53
$Ho_{0.50}La_{0.5}C_2$	"	2.7	5.2	0.52

rate constant in a series of experiments was found to be beyond the $\mp$ 15% deviation an obvious experimental anomaly was observed; for example, beads cracking open during the experiment to reveal fresh surfaces or a shiny impervious wax appearing as a surface layer. These results were then ignored in subsequent considerations.

Linear reaction kinetics were almost universally observed, at least for the first 20 min, which was the usual time interval over which the pressure rise was followed. Beyond 40 min the bead began to suffer substantial reduction in surface area which would of course influence the rate of gas evolution.

Results and Discussion

Although this paper concentrates on data obtained while studying the $Ho_{1-x}La_xC_2$ series of solid solutions, chosen because neither Ho nor La was expected to be present in oxidation states other than III, and the series from $x = 0$ to 1.0 encompasses cubic phases when $0.30 < x < 0.75$, the distribution of hydrocarbon products for the cubic phase in truly mild conditions was examined. Table I indicates that, compared to the tetragonal precursor phases, the surfaces of the cubic carbides are less catalytic or less metallic; thus more acetylene is unreduced. Shorter C–C lengths in the solid would also lead to an expectation of greater acetylene

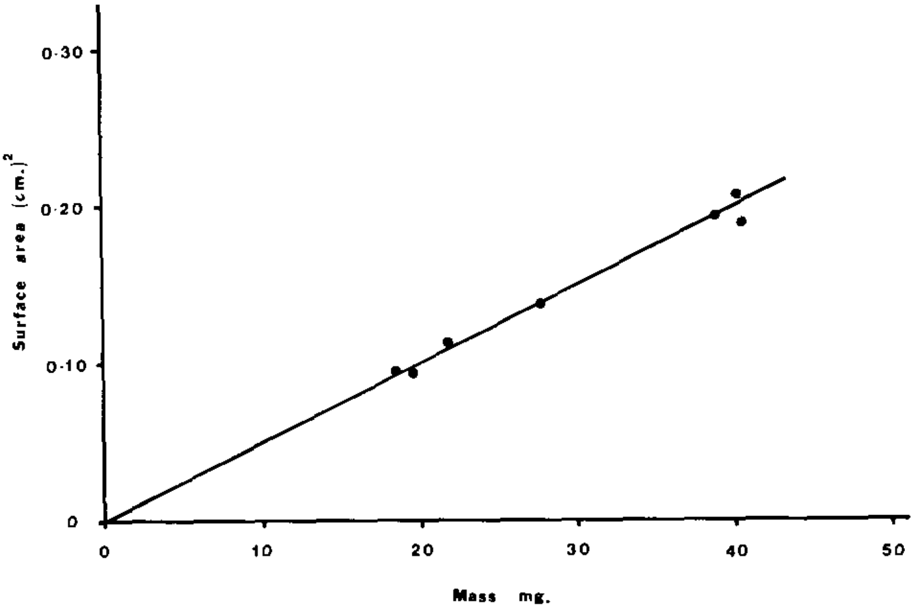

FIG. 1. The relationship between the calculated surface area of the samples used for hydrolysis and their mass.

TABLE III

LATTICE PARAMETERS OF $Ho_{1-x}La_xC_2$ SOLID SOLUTIONS

	Lattice parameters			
Composition x	a (nm	c nm)	Cell volume (nm^3)	Volume per metal atom (nm^3)
0	0.3878_2	0.6562_3	$.0987_0$	$.0493_5$
10	0.3873_9	0.6515_3	$.0977_8$	$.0488_9$
15	0.3854_5	0.6492_1	.09648	.04824
25	0.3816_5	0.64761	.09435	.04718
30	0.3775_2	0.6469_4	.09219	.04610
33	0.5801	—	.19520	.04880
40	0.57144	—	.18650	.04660
48	0.5683_7	—	.18360	.04590
50	0.5678_2	—	.18310	.04578
55	0.5652_5	—	.18060	.04510
60	0.56449	—	.17990	.04498
62	0.5637_1	—	.17913	.04478
70	0.5610_4	—	.17660	.04415
74	0.5607_4	—	.17630	.04410
78	0.3683_2	0.6192_0	.08399	.04200
80	0.3679_3	0.6182_1	.08367	.04183
85	0.3670_3	0.6171_6	.08313	.04156
90	0.36544	0.6113_6	.08163	.04081
100	0.3626_5	0.6098_3	.08022	.04011

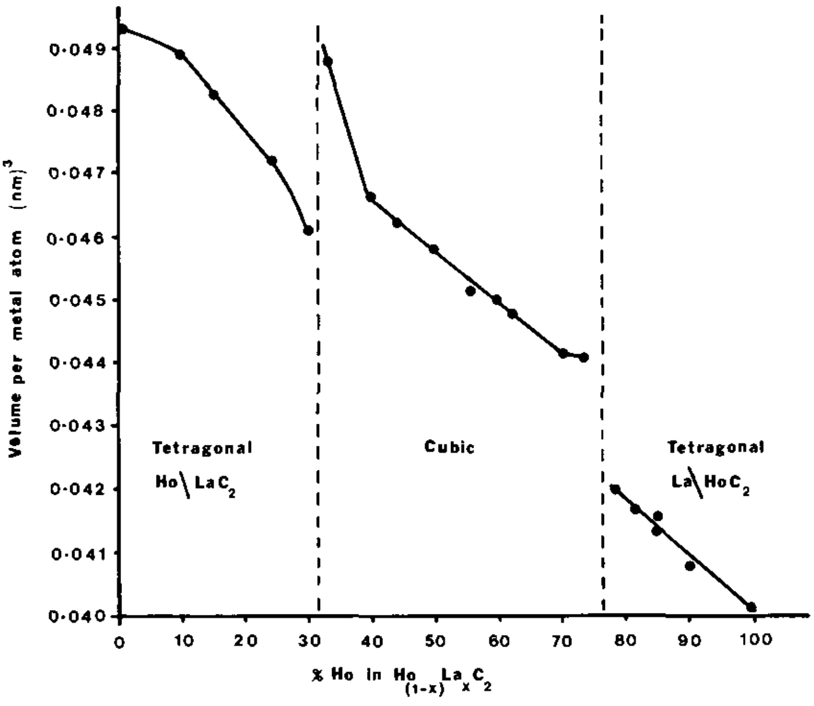

FIG. 2. Volume per metal atom in the unit cell of $Ho_{1-x}La_xC_2$ solid solutions.

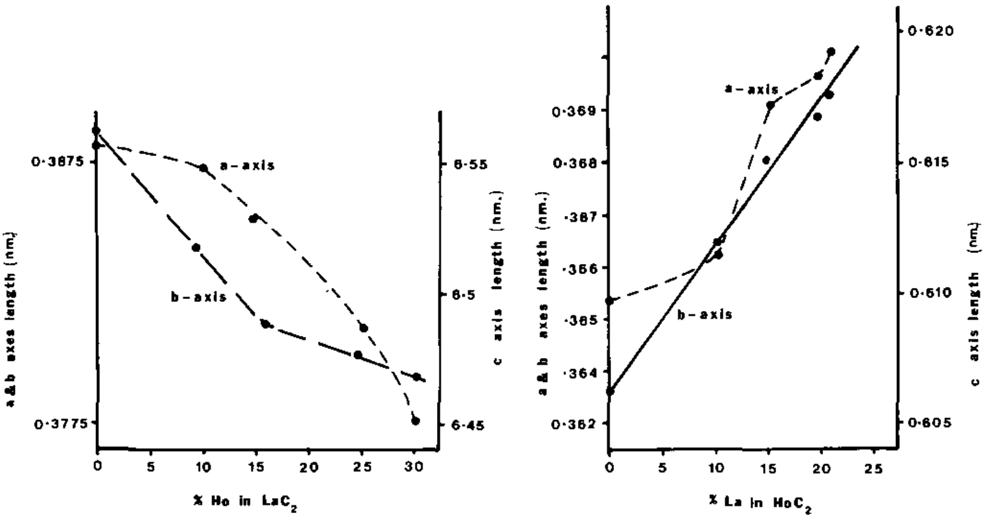

FIG. 3. Unit cell a, b, and c parameters as a function of composition in $Ho_{1-x}La_xC_2$ through the two tetragonal phase regions.

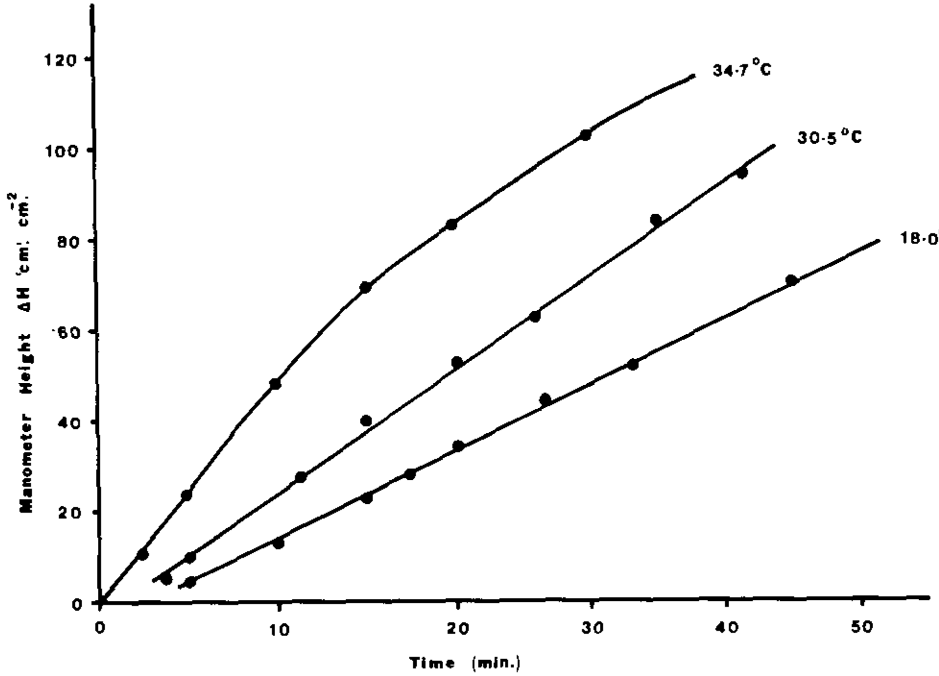

FIG. 4. Evolved gas volume as a function of time for hydrolysis of tetragonal $Ho_{0.85}La_{0.15}C_2$ at different temperatures.

evolution. Since water, not water vapor, was to be the reagent several dicarbide solid solutions were tested to see the effect this change in the conditions had. The gas volume expected from Eqs. [1] and [2] was compared to the final volume of gas obtained after the sample had been completely reacted and these results are shown in Table II; the V_0/V_e ratio is quite constant and the average value of 0.51 is the same as that found for the trivalent dicarbides in (*4*). For comparison purposes the observed linear rate constants, K_L, were multiplied by the factor $0.51/(V_0/V_e)$obs.

Each arc-melted bead made for examination had a very smooth shiny metallic surface with a shape such that the diameter of the base was always smaller than the height, indicating that each bead was something between a hemisphere and a sphere. Micrometer gauge measurements made on each bead in an argon-filled dry box were used to determine the surface area from the formula: surface area $= 3\,r^2 + 2\,rh$, where h is equal to $(H - r)$, where H was the height of the bead and r was the radius of the base of the bead. The relationship between the mass of the bead, in the range used for this work, and the estimated surface area, Fig. 1, gives an indication that the surface area estimation process was consistent and relatively accurate. Clearly, from Fig. 1 and the constancy of V_0/V_e, reasonable confidence can be placed in the observed rate constant data as a function of composition.

Some lattice parameter values are given in Table III from which the unit cell volumes were calculated and from which the volume per metal atom in the body centered tetragonal or face centered cubic unit cells was calculated.

When the X-ray results are presented as

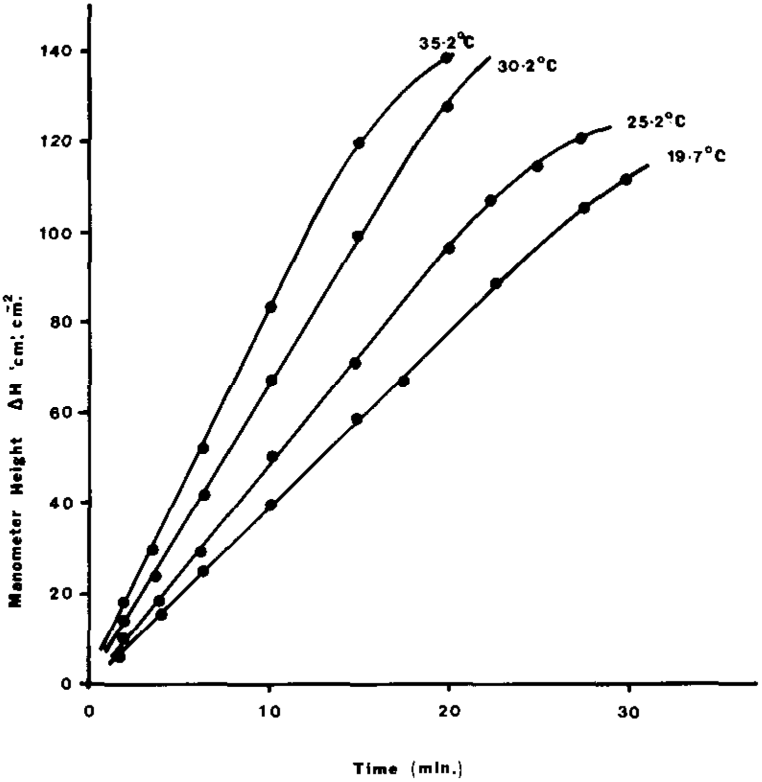

FIG. 5. Evolved gas volume as a function of time for hydrolysis of cubic $Ho_{0.4}La_{0.6}C_2$.

the volume per metal atom in the unit cell, Fig. 2, several features emerge which may bear on the subsequent hydrolysis rate data. First when the system is considered as having the small volume dicarbide, HoC_2, as a solvent for the large cell dicarbide, LaC_2, a normal solution is implied as the volume increases linearly up to 24% of Ho replacement by La. As Fig. 3 shows, this is true as far as the *a*, *b* axis expansion is concerned but not for the *c* direction, along which the C_2^{n-} dipoles are aligned in the tetragonal structure. The *c* axis expansion appears somewhat erratic with a larger expansion occurring between 10% and 15% substitution of Ho. One explanation for this could be an increase in the C–C distance along the *c* direction and such an increase can be associated with an increase in electron density in the $C_2^{n-} - p_\pi^*$ antibonding levels. It is these orbitals that are involved in M–C_2 covalent bonding. Thus an increase in C–C bond length would imply an increase in M–C_2 bonding from this covalent component and from an increase in the ionic component of bonding as n in C_2^{n-} is raised by the localization of more metal orbital density on the C_2^{n-} dipole.

Returning to Fig. 2, the increase in volume per metal atom is very sharp near the phase change. This situation is expected if the C_2^{n-} dipoles become disordered along the ⟨111⟩ directions of the cubic unit cell, where the C–C axis will be directed between metal atoms on octahedral sites. This random structure would then have decreased M–C_2 overlap with a weakening of the M–C_2 bonding and a decreased C–C distance as

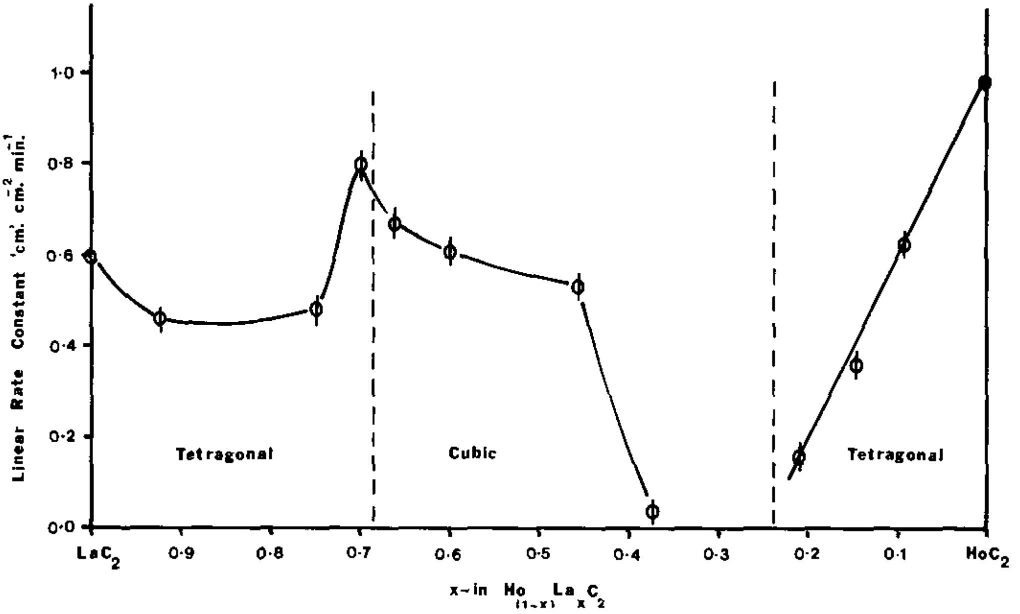

FIG. 6. Variation in linear rate constant with composition at 20°C for the $Ho_{1-x}La_xC_2$ series of solid solutions.

less electron density occurs in the antibonding levels. Increased hydrolysis reactivity might then be expected with a higher percentage of acetylene. Then with no preferred overlap direction, as more Ho is replaced by La there is a linear increase in atomic volume through most of the cubic phase as seen in Fig. 2. The linearity is sharply lost close to the cubic–tetragonal phase boundary, which mirrors the situation at the first phase boundary. When the volume per atom diagram, Fig. 2, is viewed from the larger cell volume carbide, LaC_2 acting as solvent for HoC_2, the solution looks far from ideal. The smaller diameter of Ho^{3+} initially leads to poorer metal–C_2 overlap with less electron density in the $2p_\pi^*$ levels and shorter C–C distances. However, the overall effect is masked by the La–C_2 interactions providing the skeleton of the structure. Initially the *a*, *b* parameters show only a small decrease in size, Fig. 3, while the *c* axis shows a more marked linear decrease up to 17% replacement. The *c* axis decrease arises from the C–C bond length decrease as less metal orbital 2*p* interaction populates the antibonding level. At about 30% replacement the sudden increase in volume per metal atom in the structure is in accord with a ⟨111⟩ random orientation of C_2^{n-} dipoles each with reduced M–C_2 bond strength.

The hydrolysis data can be tentatively interpreted in terms of this model, where weaker M–C_2 bonding and shorter C_2^{n-}, C–C distances emerge as solid solution proceeds with a prospective increase in reactivity when the cubic phase is encountered. Figures 4 and 5 demonstrate that linear rate kinetics apply for about 20 min of observation for both tetragonal and cubic solid solutions and that rate increases with temperature within the narrow range that could be investigated. The variation of rate with temperature enabled Ahrrenius-type plots to be

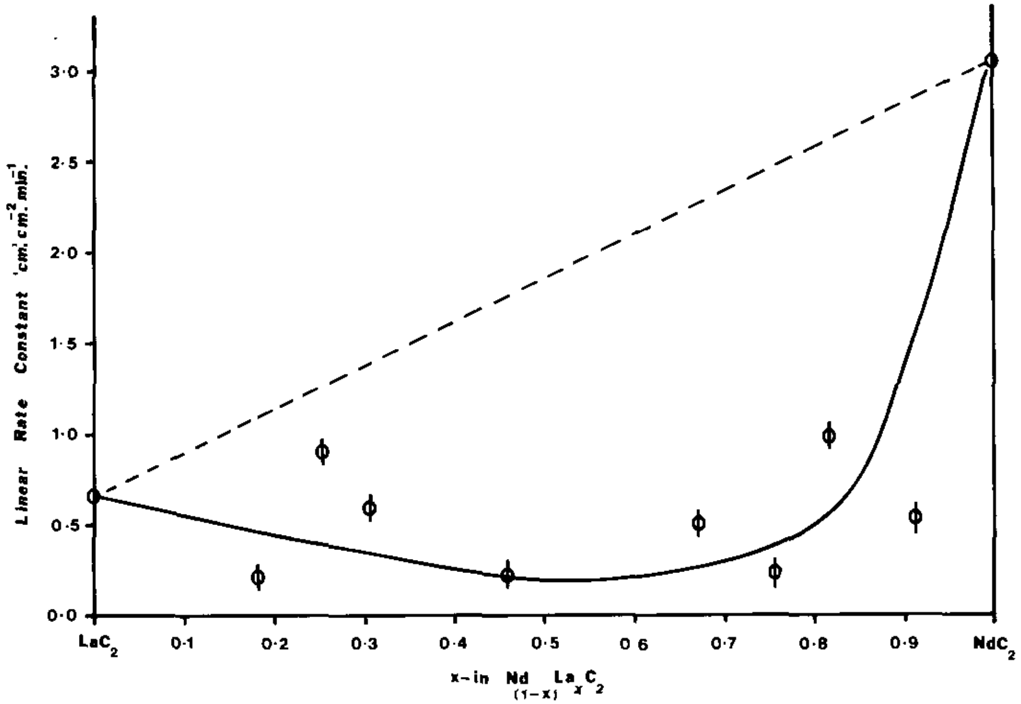

FIG. 7. Change in the linear rate constant with composition at 20°C for $Nd_{1-x}La_xC_2$ solid solutions.

made and activation energies to be estimated. Linear rate constants as a function of composition are plotted in Fig. 6 for $Ho_{1-x}La_xC_2$ alloys; they show that the reaction rate falls in the low La concentration, tetragonal range. This pattern of behavior is the mirror image of the volume per atom plot in Fig. 2 and is interpreted as an increasing M–C_2 bond strength.

Within the cubic solid-solution range there is an increase in reaction rate up to the second tetragonal phase boundary. The effect of the substitution of the small atom, Ho, for La is seen to be, from the decreased K_L values, a small increase in M–C_2 bond strength.

In order to make comparisons a series of solid solution dicarbides that were tetragonal across the whole composition range were prepared and examined. This series was $Nd_{1-x}La_xC_2$ and the linear rate constant against composition plot is shown as Fig. 7, where the only crude correlation appears to be a sharp decrease in K_L when the first La substitution for Nd is made and thereafter a range of values fluctuating around the value for LaC_2. The reaction rate constants for the tetragonal solid solutions are always below the line connecting the parent dicarbides. When this test is applied to the $Ho_{1-x}La_xC_2$ series it can be seen that the linear rate constants for the cubic solid solutions are on or above any line connecting LaC_2 to HoC_2 in Fig. 6, which suggests that the cubic phase is more reactive than the tetragonal phase.

The presence of strain energy in the tetragonal phases, which is believed (9) to be responsible for depressing the transition temperature of the cubic to tetragonal transformation, may not contribute to increasing the rate of reaction. Increased M–C_2 bonding is the main factor in the decrease.

Both these series of solid solutions have

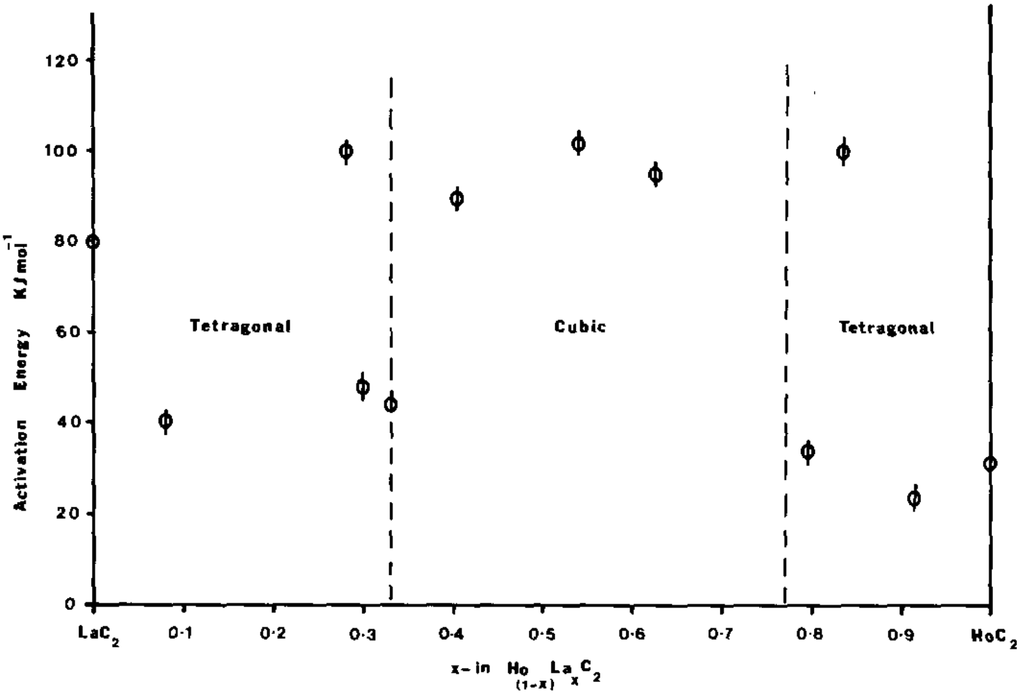

FIG. 8. Hydrolysis reaction activation energies for a series of $Ho_{1-x}La_xC_2$ solid solutions.

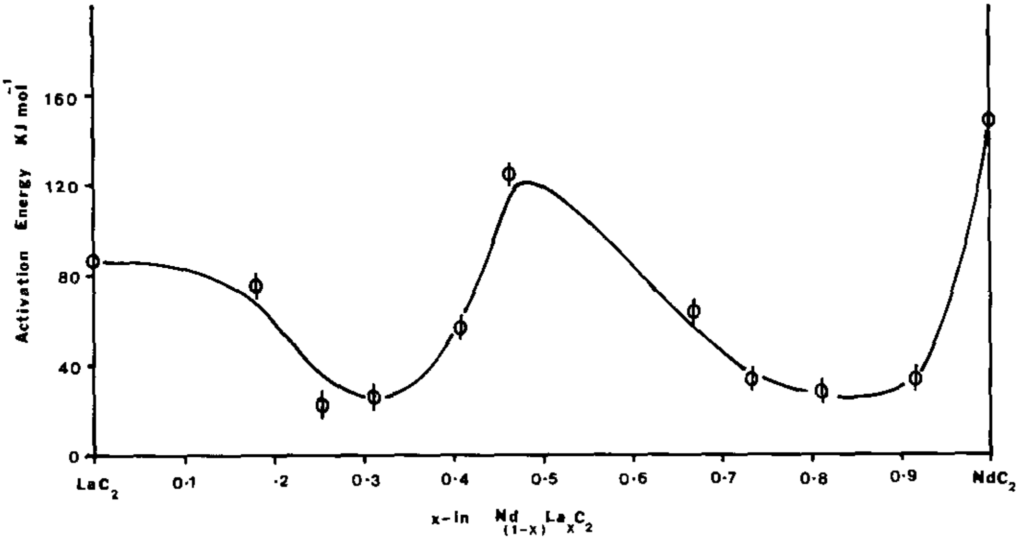

FIG. 9. Hydrolysis reaction activation energies for a series of $Nd_{1-x}La_xC_2$ solid solutions.

been the subject of a microhardness study (*10*) and it is interesting to note that Figs. 4 and 5 in Ref. (*10*), which show microhardness as a function of composition, are almost perfect mirror images of Figs. 6 and 7 here for K_L vs composition. Thus as La replaces Ho in HoC_2 there is a small decrease in hardness followed by a sharp rise to the tetragonal–cubic phase boundary. Across the cubic phase the hardness decreases as more Ho is replaced, reaching a minimum near to the next cubic–tetragonal boundary. In a simple way the K_L values are rising as the hardness of the solid is decreasing and weaker M–C_2 covalent bonding arises from the solid solution formation.

The hydrolysis reaction rate increased with temperature and within the limitations imposed by few data points, only 4 or 5 per sample, ln K_L v $1/T$ plots were linear. The activation energies shown in Figs. 8 and 9 were obtained from these plots. From the erratic looking plot it is only possible to speculate that tetragonal solid solutions have lowered activation energies, possibly due to the presence of the strain energy component. Some of the confusion in the data appears in the region of the phase change boundaries, but in general cubic solid solutions have a significantly higher activation energy for the reaction. This would imply a changed rate determining step for the cubic as compared to the tetragonal phases.

With the exception of the $Nd_{0.45}La_{0.5}C_2$ sample it appears that again substantial decreases in activation energy are encountered when solid solutions in this series undergo hydrolysis. This picture, presented in Fig. 9, supports the view that a significantly changed rate controlling step arises from the randomly oriented C_2^{n-} dipoles being involved in the hydrolysis reaction of the cubic phases in the $Ho_{1-x}La_xC_2$ series and that strain energy possibly contributes to the reaction of the solid solutions.

Summary

Linear reaction rate constants have been measured for the hydrolysis reaction of two series of solid solutions. From comparison of the way the K_L values change with composition and from activation energy measurements, a different rate controlling step occurs in the cubic solid solutions compared to the tetragonal ones. The way in which unit volume per metal atom and a and c axes change with composition indicate that the cubic phase is formed when aligned C_2^{n-} dipoles reorient randomly along the $\langle 111 \rangle$ directions.

Reaction rate data and microhardness measurements are in agreement with predictions concerning the M–C_2 bonding changes as metal s–p–d–f orbitals and C_2^{n-} $2p_\pi^*$ orbitals produce a covalent component in the bonding in these systems.

References

1. J. S. Anderson, N. J. Clark, and I. J. McColm, *J. Inorg. Nucl. Chem.* **30**, 105 (1968).
2. N. J. Clark and I. J. McColm, *J. Inorg. Nucl. Chem.* **34**, 117 (1972).
3. I. J. McColm and T. Q. Quigley, *J. Less-Common Met.* **169**, 347 (1991).
4. I. J. McColm, T. A. Quigley, and D. R. Bourne, *J. Less-Common Met.* **170**, 191 (1991).
5. J. S. Anderson, N. J. Clark, and I. J. McColm, *J. Inorg. Nucl. Chem.* **31**, 1621 (1969).
6. I. J. McColm, I. Colquhoun, and N. J. Clark, *J. Inorg. Nucl. Chem.* **34**, 3809 (1972).
7. I. J. McColm, T. A. Quigley, and N. J. Clark, *J. Inorg. Nucl. Chem.* **35**, 1931 (1973).
8. A. Schurenkamper, *J. Inorg. Nucl. Chem.* **32**, 417 (1971).
9. I. R. Loe, I. J. McColm, and T. A. Quigley, *J. Less-Common Met.* **46**, 217 (1976).
10. I. J. McColm, *J. Less-Common Met.* **78**, 287 (1981).